Journal of Coastal Research	22	3	645–663	West Palm Beach, Florida	May 2006

Application of a Cross-Shore Profile Evolution Model to Barred Beaches

Mohamed A.K. Elsayed

Department of Engineering Science and Mechanics
Virginia Tech
Mail Code (0219)
Blacksburg, VA 24061, U.S.A.
melsayed@vt.edu

ABSTRACT

ELSAYED, M.A.K., 2006. Application of a Cross-Shore Profile Evolution Model to Barred Beaches. *Journal of Coastal Research,* 22(3), 645–663. West Palm Beach (Florida), ISSN 0749-0208.

A cross-shore profile evolution model, Uniform Beach Sediment Transport-Time-Averaged Cross-Shore (UNIBEST-TC), is used in the present study. The model was developed at WL/Delft hydraulic laboratory in the Netherlands and comprises a conglomerate of submodels representing identified processes of cross-shore sediment transport. Validation of UNIBEST-TC was carried out using the collected field data at the Egmond site in the Netherlands and at the Duck site in the US. The model is capable of predicting wave height and wave direction for both sites (Egmond site and Duck site). The prediction of long-shore current is reasonable for the Egmond site, but it is unsatisfactory for the Duck site. The difference between the measured and the predicted values for long-shore current and cross-shore current is partly due to the difference between the measured values, which are at a certain depth, and the predicted values that are depth-averaged velocity. Beside that, the turbulence in the breaker zone leads to errors in the measurements, which could be another factor. It is shown in the present study that on relative small scales, opposite morphological behavior is present. Therefore, morphodynamic profile modeling requires a representative characteristic bottom profile. To achieve a qualitative data for the calibration of the model, it is suggested that field measurements should include error ranges. Furthermore, the effect of small variations of the water depth on the processing of the signals should also be taken into account.

ADDITIONAL INDEX WORDS: *Hydrodynamics, orbital velocity, cross-shore current, long-shore current, morphology.*

INTRODUCTION

Research on long-shore sediment transport has been carried out extensively during the past three decades, but in recent years, emphasis is paid on the research of cross-shore sediment transport, together with the shore transformation in cross-shore direction. Long-shore transport can be regarded as better explored than cross-shore transport because it is easier to be described because of its steady nature, despite some minor unsteady influence from shear instabilities and so on. While cross-shore sediment transport is rather complex because it is strongly unsteady, the oscillatory transport components are most important.

Limited knowledge is available about cross-shore processes. Therefore, the model developers are facing a difficult task to develop their models with the limited knowledge available. Techniques have to be introduced to mitigate the present difficulties associated with modeling calibration. With this approach, UNIBEST-TC has undergone several major revisions during the past few years.

Depending on the concepts and background of their development, cross-shore profile models can be classified into four categories (ROELVINK and BROKER, 1993):

- Descriptive models. These models have been developed based on the knowledge acquired by practical observations of beaches and transformation of one beach state to another due to environmental changes.
- Equilibrium profile models. These models are based on large numbers of scale experiments and practical measurements. The basis is that beaches tend to reach equilibrium state after a storm event.
- Empirical profile evolution models. This is an extension of equilibrium models by including empirical equations to describe the profile evolution toward the equilibrium.
- Process-based models. These are deterministic types of models based on physical processes related to coastal sediment transport and combining them together with the help of the knowledge acquired so far.

The present study focuses on process-based models. Examples of process-based cross-shore models are LITCROSS (Danish Hydraulic Institute, Denmark), COSMOS 1D (Hydraulic Research Wallingford Ltd, UK), WATAN-3 (University of Liverpool, UK), SEDITEL (Laboratorie National d'Hydraulique, France), and REPLA SOGREAH (France). The scientific description and the governing equations of these process-based models are given in FREDSOE (1984), DEIGAARD, FEDSOE, and HEDEGAARD (1986), DEIGAARD and FREDSOE (1989), LONGUET-HIGGINS (1953), SVENDSEN (1984), ENGELUND and FREDSOE (1976), HEDEGAARD, DEIGAARD, and FREDSOE (1991), BATTJES and JANSSEN (1978),

DOI:10.2112/03-0096.1 received 6 May 2004; accepted in revision 17 May 2004.

Table 1. *Initial parameters setting for UNIBEST-TC (Egmond site).*

General parameters	Maximum relative wave period (s)	40
	Temperature of water (°C)	10
	Salinity of water (‰)	0
Wave-related parameters	α—wave-breaking parameter for dissipation (−)	1.0
	γ—depth limitation of maximum wave height (−)	0.60
	β—slope of wave front (m)	0.05
	f_w—friction factor for wave dissipation due to bottom friction (m)	0.01
	C_r—correlation coefficient for wave envelope and bound long waves (−)	0.25
	Breaker delay factors	λ = 2.0 *P* = 1.0
Current-related hydrodynamic parameters	α_w—viscosity coefficient for vertical velocity profile (−)	0.10
	Kc—friction factor for mean current computation (m)	0.01
Grain size parameters	D_{50} (m)	0.0003
	D_{90} (m)	0.0006
	D_{ss} (m)	0.00017
Transport parameters	Tan ϕ1—internal friction angle to correct the transport rates according to the slope at a seaward location (−)	0.03
	Tan ϕ1—internal friction angle to correct the transport rates according to the slope at a shoreward location (−)	0.10

Table 2. *Offshore boundary conditions at 5 km from shore (wave buoy at Egmond site).*

Offshore Wave and Tide Data at 5 km From the Coast	Case 1	Case 2	Case 3
Hrms (m)	1.25	1.13	0.77
Peak wave period (s)	6.67	6.25	4.55
Incident wave angle to north (°)	341.242	338.3	334.7
Incident wave angle to coast normal (°)	−63.912	−60.97	−57.37
Tide level to mean sea level (m)	0.8	−0.06	0.7

De Vriend and Stive (1987), Bailard (1981), Southgate and Nairn (1993), Isobe and Horikawa (1982), Swart (1978), Watanabe and Dibajnia (1988), Watanabe, Hara, and Horikawa (1984), Lepeintre *et al.* (1991), Fornerio and Hamm (1992), Weggel (1972), Sakai *et al.* (1988), Mase and Iwagaki (1982), and Mizuguchi (1982) and are not repeated here. The main goals of the present study are the following:

- To validate the UNIBEST-TC model by comparing model results with the measured data in the Egmond site in the Netherlands and the Duck site in the US
- To provide model developers with useful information that can be used for further improvements of the model in areas of poor performance by applying new theories and expanding the limitation of applicability

COLLECTED DATA

Egmond Site

The field site in Egmond is a coastal area of about 1 km along shore and about 1 km offshore. It is situated south of the village of Egmond aan Zee in the Netherlands. Longshore differences in the offshore wave climate are small because of the relative uniform orientation of this stretch of the Dutch coast. The wave climate is dominated by wind waves related to low-pressure areas moving from west (Atlantic) to east (European Continent). The tidal range near Egmond varies between 1.2 m (neap tide) and 2.1 m (spring tide). At the site, the flood tide has a duration of 4 to 5 hours and the ebb tide of 7 to 8 hours. The horizontal tide runs ahead of the vertical tide by about 30 to 45 minutes. The semidiurnal tide induces asymmetrical long-shore currents, which may reach values of 0.6 to 1.0 m/s. The data set (all measured data) for the event of 30 April 1998 to 5 May 1998 was available as an Excel file prepared by Delft Hydraulics within the COAST3D project. The measurements can be summarized as follows:

- Data for wave propagation model (wave height, wave direction and wave period)
- Data for flow model (long-shore current and cross-shore current)
- Data for near-bed orbital velocity model (rms·orbital velocity)
- Measured profiles for morphological runs

Initial parameters setting for UNIBEST-TC and offshore boundary conditions at the Egmond site are given in Tables 1 and 2, respectively.

Duck Site

Many studies have been carried out in order to interpret the behavior of the bar system in the surf zone of Duck beach in the US. Lippmann, Holman, and Hathaway (1993) studied the bar system (consisting of one or two shore-parallel bars) in the surf zone of Duck beach, North Carolina, U.S.A, over long-term periods. The beach and foreshore are rather steep (1–12) and consist of a mixture of medium/coarse sand with median diameters between 0.5 and 1 mm and carbonate shell debris up to 20%. Offshore, the bottom slope approaches to about 1 to 160 at the −8-m contour, and the median grain size decreases to 0.1 mm. The surf zone at Duck is characterized by a persistent, very dynamic inner bar, approximately 30 to 120 m offshore of the shoreline with the bar crest between −1 and −3 m (bar height of 1–2 m) and by a low-amplitude outer bar approximately 300 to 400 m offshore. The dune height is about 7 m; the beach width is 20 to 45 m, and the tidal range is about 1 m. The position of the inner bar was sampled on a nearly daily basis using a video method. The outer bar was surveyed by using the Crab (amphibious buggy) in combination with an automatic tracking/sounding system.

Larson and Kraus (1992, 1994) and Birkemeier (1984) studied the temporal and spatial scales of beach profile change and bar characteristics at Duck beach based on 11-year time series of high-resolution beach profile surveys. The bar characteristics were determined with respect to an adopt-

Table 3. *Bar characteristics of surf zone (Duck site).**

Bar	Sand Size (mm)	Tidal Range (m)	Slope of Surf Zone	Bar Characteristics: Height (m)	Length (m)	Volume (m^3/m)	Crest Depth to Mean Sea Level (m)	Long-Term Migration Speed: Onshore (m/d)	Offshore (m/d)
Duck	0.5–1	1	1:160						
Inner bar				0.9 (0.2/1.4)	95 (35/280)	45 (6/102)	1.6 (0.5/2.5)	0.4	0.3
Outer bar				0.4 (0/1.4)	170 (25/280)	45 (0/120)	3.8 (1.3/5.1)	0.4	0.4

* Minimum and maximum values are given in parentheses. Migration speeds are mean net long-term values (over months for onshore direction; over years for offshore direction); maximum values may be considerably high.

ed long-term equilibrium profile. The most important findings are the following:

- Most of the profile changes occur landward of the −4-m depth contour, in which zone the standard deviation of the depth to mean sea level is 0.1, 0.6, and 0.7 m for depths of 8, 4, and 1 m.
- Most of the surveyed profiles showed two bars: a pronounced inner bar and a lower but wider outer bar (see Table 3); occasionally, a triple bar was observed.
- Onshore movement of the inner bar generally is associated with an increase of volume and offshore movement with a decrease of volume; onshore movement of the outer bar is associated with a decrease of the bar volume and offshore movement with an increase of volume.
- Inner bar variability is rather large (see Table 3); maximum and minimum values of bar height, length, and volume were two to three times larger than the average values. Short-term offshore-directed bar migration speeds (defined as distance moved over period between two consecutive surveys) are as large as 20 m/d; long-term net offshore-directed migration speeds are about 0.3 to 0.4 m/d (see Table 3).
- The inner bar disappeared by moving offshore, by welding to shore, by flattening out; cycle time is about 3 years.
- The outer bar disappeared by flattening out during extended periods of low waves; the outer bar showed a gradual onshore movement (85 m over 6 mo) and disappeared as a result of steady onshore transport; cycle time is about 3 years.
- Seasonal variations in profile morphology are distinct; the summer average profile is highest (maximum amount of sand) between the −1- and −3-m contour lines; the summer average profile is lowest between the −3- and −4-m lines.
- There is a slight tendency that onshore movement of the inner bar corresponds to seaward movement of the shoreline (Birkemeier, 1984).

The data set for the Duck site used in this study has been given for two periods: (i) 10 to 20 October 1998 (offshore bar migration) and (ii) 22 to 27 September 1998 (onshore bar migration).

- The measurements can be summarized as follows: data for wave propagation model (wave height, wave direction, and wave period), data for flow model (long-shore current and cross-shore current), and measured profiles for morphological runs.

ANALYSIS METHOD

UNIBEST-TC Model

The model consists of a combination of several submodels. Basic mathematical formulations of each submodel are given here. For more description, the reader is referred to Bosboom *et al.* (1997).

Wave Propagation Model

The wave propagation model calculates the wave energy decay along a cross-shore ray, including the effects of shoaling, refraction, and energy dissipation. Many previous studies showed that the wave propagation model is performing well. The model consists of three first-order differential equations as follows:

- The time averaged wave energy balance (Battjes and Janssen, 1978):

$$\frac{\partial}{\partial x}[EC_g \cos\,\theta] = -D_w - D_f \tag{1}$$

where

x = cross-shore direction
E = organized wave energy (J/m^2)
C_g = wave group velocity (m/s)
D_w = dissipation of wave energy due to wave breaking (J/m^2)
D_f = dissipation of wave energy due to bottom friction (J/m^2)

- The balance equation for energy contained in surface rollers in breaking waves follows:

$$\frac{\partial}{\partial x}[2E_r C \cos\,\theta] = D_w - \text{Diss} \tag{2}$$

where

E_r = roller energy representing the amount of kinetic energy in the roller
Diss = dissipation of roller energy

• Horizontal momentum balance from which the mean water level setup is computed through the following:

$$\frac{\partial \eta}{\partial x} = -\frac{1}{\rho g h}\frac{\partial S_{xx}}{\partial x} \quad (3)$$

where

η = water surface elevation above mean sea level (m)
S_{xx} = radiation stress in the cross-shore direction
h = water depth measured from mean surface level (m)
g = gravitational acceleration (m/s^2)

Mean Current Profile

The gradient of the depth-integrated cross-shore radiation stress is balanced by wave setup, whereas long-shore radiation stress gradient is balanced by a time mean bed shear stress associated with a long-shore current. The cross-shore circulation current is generated because of the imbalance between the cross-shore radiation stress and the pressure gradient due to setup, which causes a shoreward mass flux above the trough of the waves and a return flow in seaward direction below the trough level.

To obtain the distribution of long-shore currents and the circulation current, a quasi-3D model according to De Vriend and Stive (1987) is used. This model takes into account the presence of wind-shear stresses, breaking-induced forcing, and surface layer and wave boundary layer. A parabolic viscosity distribution is used in order to combine the effect of turbulence from different sources in a consistent manner. The model for mass flux due to surface rollers and nonbreaking progressive waves in the surf zone is ill predicting, or the model for the return flow due to those mass fluxes is ill predicting. For the time being, the mass flux induced return flow has to be calculated in different ways in different regions in the cross-shore profile.

Near-Bed Orbital Velocity

The orbital velocity required for the sediment transport calculation is represented as a time series. Therefore, a time series is produced having the same characteristics of asymmetry, bound long waves and amplitude modulation as in a random wave field. The orbital velocity model consists of two parts:

• Contribution due to the wave asymmetry computed for monochromatic waves, where mean wave energy and peak period is used as input parameters for random waves.
• Contribution due to bound long waves and an empirical relationship for the phase of a bound long wave relative to the short-wave envelope. The final computation of orbital velocity is obtained by adding the contribution from the short-wave envelope and the bound long-wave contribution. The prediction of orbital velocity is overestimated. Therefore, the relation between wave envelope for short waves and bound long wave needs to be revised.

Sediment Transport Models

Separate formulations are used for bed load transport and suspended load transport. Here bed load means that the particles are more or less continuously in contact with the bed.

Bed Load Transport: Movement of bed load is presented in two ways in the formulations: at small shear stresses individual particles move along the rippled bed, and at higher shear stresses the particles move over the bed in several layers as a sheet flow. The nondimensional instantaneous bed load transport vector according to Van Rijn *et al.* (1995) is given by

$$\varphi_{bd}(t) = \frac{q_b(t)}{\sqrt{\Delta g d_{50}^3}} = 9.1\frac{\beta_s}{(1-p)}[\theta'|(t)| - \theta_{cr}]^{1.8}\frac{\theta'(t)}{|\theta'(t)|} \quad (4)$$

where

t = time (s)
q_b = bed load transport rate in volume per unit time and width including pores (mm^3/m/s)
d_{50} = median grain diameter (m)
Δ = relative density = $(\gamma_s - \gamma)/(\gamma)$ $(-)$
g = gravitational acceleration (m/s^2)
θ_{cr} = dimensionless critical shear stress $(-)$
θ' = dimensionless effective shear stress $(-)$
β_s = slope factor $(-)$
p = porosity of the sediments $(-)$
γ_s = density of sediments (= 2,650 kg/m^3)

The instantaneous cross-shore and long-shore transport components are obtained from the following equations:

$$q_{bx} = \frac{u_{bx}}{|u_b|}q_b \quad (5)$$

$$q_{by} = \frac{u_{by}}{|u_b|}q_b \quad (6)$$

where

x = long-shore component
y = cross-shore component
u_b = time-dependent near-bed horizontal velocity vector (m/s)
u_{bx} = x-component of vector u_b (m/s)
u_{by} = y-component of vector u_b (m/s)
q_b = bed load transport vector (m^3/m/s)

The net wave-averaged bed load transport rate is obtained by averaging the time-dependent transport vector $q_b(t) = (q_{bx}, q_{by})$ over the duration of the near bottom velocity time series. The bed forms have a significant influence on sediment transport processes. Sometimes the direction of transport may reserve because of the presence of the bed forms. This feature is so far not taken into account in UNIBEST-TC.

Suspended Load Transport: The suspended sediment transport rate is the product of concentration vertical and the velocity vertical:

$$q_s = \int_a^{h+\eta} VC\, dz \quad (7)$$

where

V = local instantaneous fluid velocity at height z above bottom (m/s)
C = local instantaneous sediment concentration at height z above bottom (kg/m^3)

h = water depth measured from mean surface level (m)
η = water surface elevation (m)
a = thickness of bed load layer (m)
v = time- and space-averaged fluid velocity at height z above bottom (m/s)
c = time- and space-averaged concentration at height z above bottom (kg/m^3)

The two components for time-averaged wave-related sediment transport rate ($q_{s,w}$) and time-averaged current related sediment transport rate ($q_{s,c}$) are as follows:

$$\overline{q_{s,w}} = \int_a^h \overline{\overline{vc}}\, dz \tag{8}$$

$$\overline{q_{s,c}} = \int_a^h \overline{vc}\, dz \tag{9}$$

The suspended sediment transport rate with the porosity factor is given by

$$\overline{q_{s,c}} = \int_a^h \frac{vc\, dz}{(1-p)\rho_s} \tag{10}$$

The time-averaged concentration profile is calculated by the convection-diffusion equation (assumed to be valid for wave related mixing):

$$w_{s,m}c + \varphi_d \epsilon_{s,cw}\frac{dc}{dz} = 0 \tag{11}$$

where

$w_{s,m}$ = fall velocity of suspended sediment in a fluid sediment mixture (m/s)
$\epsilon_{s,cw}$ = sediment-mixing coefficient for combined current and waves (m^2/s)
c = time-averaged concentration at height z above the bed (kg/m^3)
ϕ_d = damping factor depending on the concentration (−)

Bed Level Model

The bed level changes due to both suspended and bed load transport taking into account waves and currents are computed by the depth-integrated mass balance equation;

$$\frac{\partial Z}{\partial t} + \frac{\partial q_{bot+sus}}{\partial x} = 0 \tag{12}$$

where

Z = bed level with respect to a reference level

Validation of the UNIBEST-TC Model for the Egmond Site

The values of input parameters for the UNIBEST-TC model for the Egmond site are given in Table 1. Hydrodynamic runs are carried out for both the whole time series and for some specific runs. Table 2 gives the offshore boundary conditions for the three selected hydrodynamic runs. The average profile of 1 May 1998 in the Egmond area is used as an initial profile to predict the shape of the profile after 5 days for two cases:

Table 4. *Parameters setting for boundary conditions (Duck site).*

General parameters	Maximum relative wave period (s)	40
	Temperature of water (°C)	10
	Salinity of water (‰)	30
Wave-related parameters	α—Wave-breaking parameter for dissipation (−)	1.0
	α—Depth limitation of maximum wave height (−)	0.60
	β—Slope of wave front (m)	0.1
	f_w—friction factor for wave dissipation due to bottom friction (m)	0.01
	C_r—correlation coefficient for wave envelope and bound long waves (−)	0.25
	Breaker delay factors	$\lambda = 2.0$ $P = 1.0$
Current-related hydrodynamic parameters	α_w—viscosity coefficient for vertical velocity profile (−)	0.10
	Kc—friction factor for mean current computation (m)	0.01
Grain size parameters	D_{50} (mm)	0.2 | 0.5
	D_{90} (mm)	0.3 | 0.6
	D_{ss} (mm)	0.2 | 0.4
Transport parameters	Tan ϕ1—internal friction angle to correct the transport rates according to the slope at a seaward location (−)	0.03
	Tan ϕ1—internal friction angle to correct the transport rates according to the slope at a shoreward location (−)	0.10

- The measurements of wave heights, wave directions, and peak wave periods for a time series of 5 days
- Storm condition with constant wave height (Hs = 1.7 m, wave direction = −60°, Tp = 7.5 s)

Validation of the UNIBEST-TC Model for the Duck Site

The values of input parameters for the UNIBEST-TC model for the Duck site are given in Table 4. Hydrodynamic runs have been made every 6 hours for the available data at the Duck site during the two following periods: (i) 10 to 20 October 1998 and (ii) 22 to 27 September 1998. For morphodynamic runs, the measured profile of October 1998 at the Duck site is used as an initial profile to predict the shape of the profile after 10 days. Also, the measured profile of 21 September 1998 at the Duck site is used as an initial profile to predict the shape of the profile after 5 days.

RESULTS

Results of Specific Runs at the Egmond Site

Case 1

This case has the following characteristics; high water at t = 69 hours, Hrms (root-mean-square wave height) = 1.25 m. Figure 1 gives the computed and the measured wave height, long-shore current, and orbital velocity for the aver-

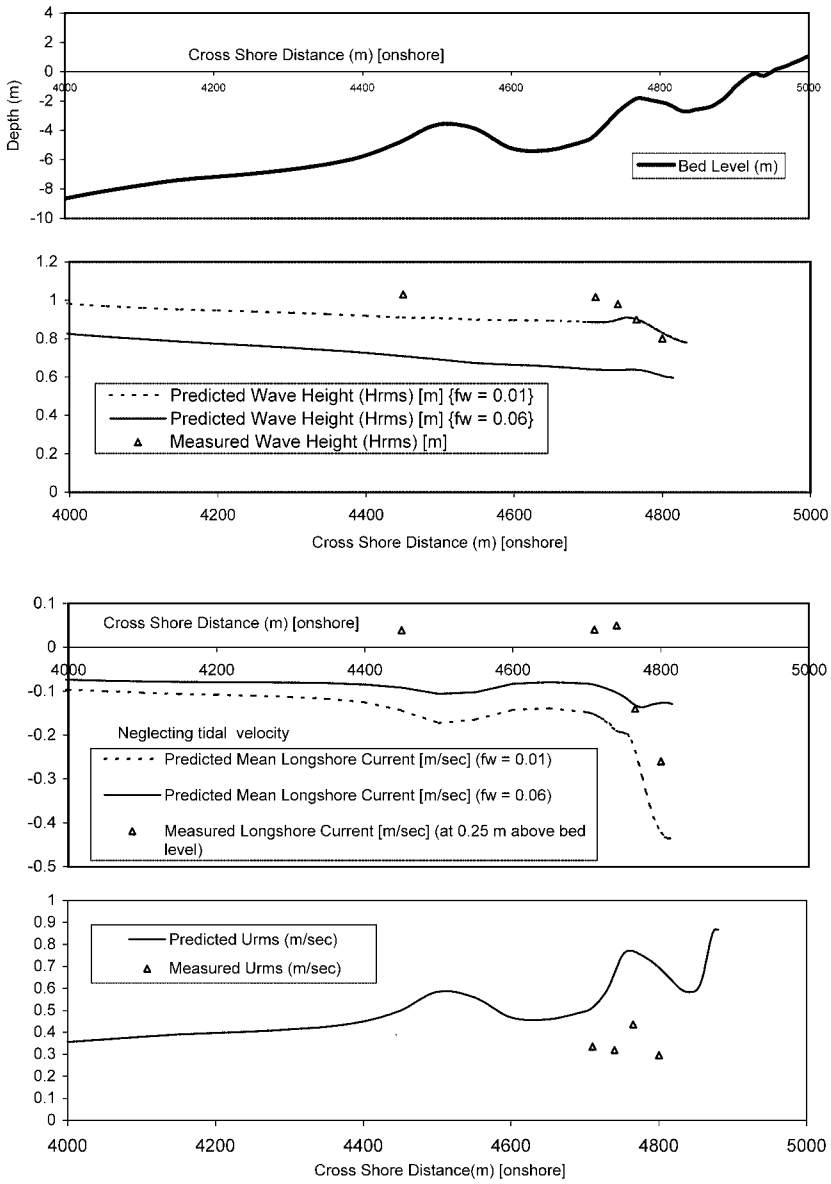

Figure 1. Comparison between measured and predicted values of wave height, long-shore current, and near-bed orbital velocity (Egmond site, case 1, after 69 h).

age profile of 1 May 1998. The effect of spatial variations on the computed results has been taken into account by making runs for different profiles (mean bed level and those including $\pm$ standard error). Figure 2 gives the distribution of wave height and long-shore current along the profile using three profiles: (i) average profile of 1 May 1998, (ii) average profile of 1 May 1998 + σ (standard deviation), and (iii) average profile of 1 May 1998 $-$ σ.

Wave Height: The distribution of the wave height along the profiles shows the following:

- The computed values are smaller than the measured values about 15% in the stations seaward of the middle bar.
- There is a good agreement between the computed values and the measured values in the inner slope of the middle bar.
- Most of the wave breaking occurs on top of the middle bar where the water depth is about 2.3 m; the waves approaching the bar have a height of about 1.0 m, resulting in a wave height of about 0.43 m.
- Using $f_w = 0.06$ (the friction factor for wave dissipation due to bottom roughness) gives an underestimation of the wave height.
- Using three profiles, the possible errors of the computed wave height can be obtained.

Mean Long-shore Current Below Wave Trough: The effect of tidal velocity and the bed roughness are given here:

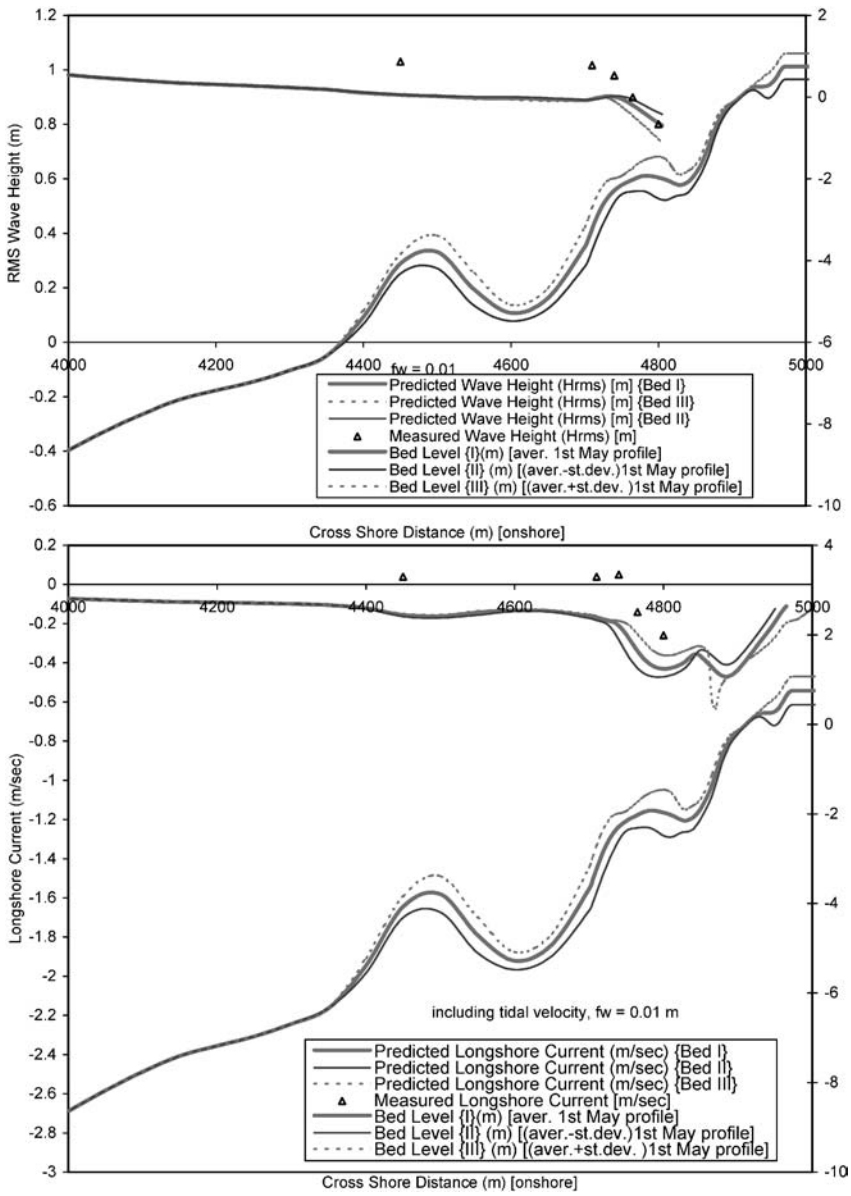

Figure 2. Comparison between measured values and predicted values of wave height and long-shore current using different profiles (Egmond site, case 1, after 69 h).

- Excluding tidal velocity leads to underestimation of long-shore current calculated by the model.
- There is a good agreement between measured and computed values for the case of including tidal velocity, especially for the case of using (average profile + σ).
- $f_w = 0.06$ gives underestimation of the computed long-shore currents.

Orbital Velocity (Urms): The computed values overestimate the measured values because the orbital velocity gives cross-shore activity and improvement of the used theory for calculating the effect of wave asymmetry is needed.

Case 2

This case is corresponding to the conditions of low water at $t = 72$ hours and Hrms = 1.13 m. Figure 3 gives the computed and the measured wave height, long-shore current, and orbital velocity for the average profile of 1 May 1998. Also, Figure 4 gives the distribution of wave height and long-shore current along the profile using three profiles: (i) average profile of 1 May 1998, (ii) average profile of 1 May 1998 + σ, and (iii) average profile of 1 May 1998 − σ.

Wave Height: The distribution of wave heights along the profiles shows the following:

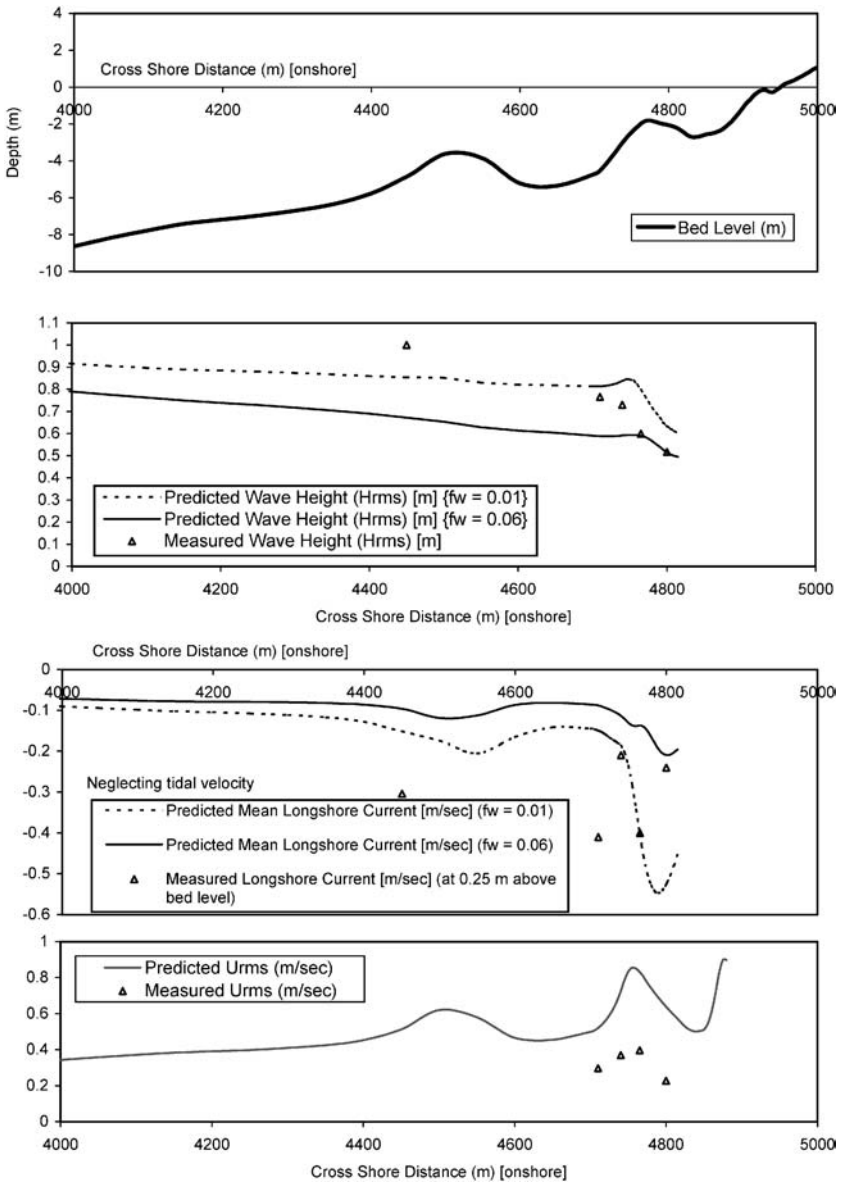

Figure 3. Comparison between measured and predicted values of wave height, long-shore current, and near-bed orbital velocity (Egmond site, case 2, after 72 h).

- The computed values are larger than the measured values about 10% in the stations seaward of the middle bar and also 10% larger for the stations in the inner slope of the middle bar.
- Most of the wave breaking occurs on top of the middle bar where the water depth is about 1.44 m; the waves approaching the bar have a height of about 0.8 m, resulting in a wave height of about 0.55 m.
- Using $f_w = 0.06$ (the friction factor for wave dissipation due to bottom roughness) gives an underestimation of the wave height for the stations seaward of the middle bar. But there is a good agreement between the computed values and the measured values in the stations in the inner slope of the middle bar.
- Using three profiles show that there is a good agreement between the computed values and the measured values by considering the case (average profile + σ).

Mean Long-Shore Current Below Wave Trough: The effect of tidal velocity is summarized as follows:

- Neglecting tidal velocity leads to overestimation of the computed long-shore current for the case of $f_w = 0.06$, whereas, using $f_w = 0.01$ gives better agreement between the measured and the computed values.

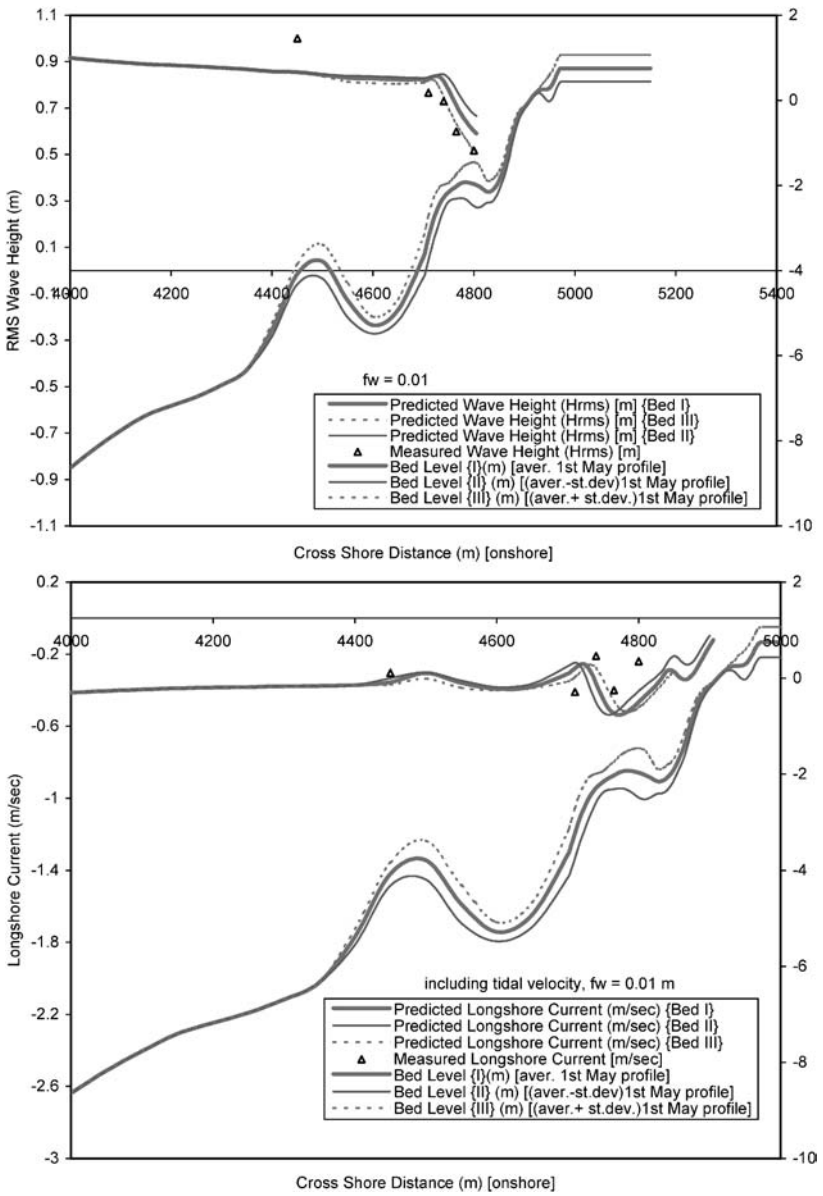

Figure 4. Comparison between measured values and predicted values of wave height and long-shore current using different profiles for Egmond site (case 2, after 72 h).

● Including tidal velocity gives a good agreement between the computed and the measured long-shore current, especially for the case (average profile + σ).

Orbital Velocity (Urms): The model always overestimates the orbital velocity.

Case 3

This case is corresponding to the conditions of high water at t = 78 hours, Hrms = 0.77 m. Figure 5 shows the computed and the measured wave height, long-shore current, and orbital velocity for the average profile of 1 May 1998, whereas Figure 6 gives the distribution of wave height and long-shore current along the profile using three profiles: (i) average profile of 1 May 1998, (ii) average profile of 1 May 1998 + σ, and (iii) average profile of 1 May 1998 − σ.

Wave Height: The distribution of wave heights along the profiles shows the following:

● The computed values are larger than the measured values about 5% in the stations seaward of the middle bar and also 5% larger for the stations in the inner slope of the middle bar.

● Most of the wave breaking occurs on top of the middle bar

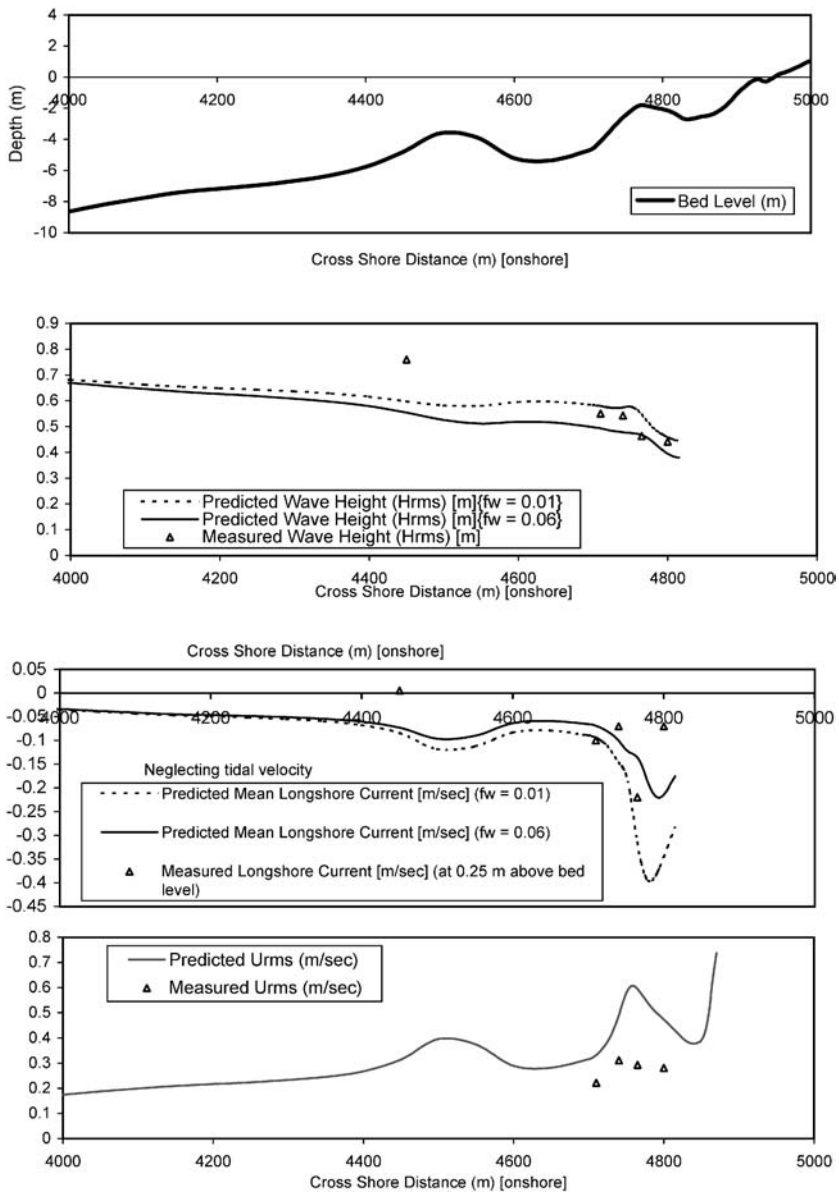

Figure 5. Comparison between measured and predicted values of wave height, long-shore current, and near-bed orbital velocity (Egmond site, case 3, after 78 h).

where the water depth is about 2.2 m; the waves approaching the bar have a height of about 0.6 m, resulting in a wave height of about 0.27 m.

- Using $f_w = 0.06$ (the friction factor for wave dissipation due to bottom roughness) gives an underestimation of the wave height.
- Using three profiles show that there is a good agreement between the computed values and the measured values by considering the case (average profile + σ).

Mean Long-Shore Current Below Wave Trough: The effect of tidal velocity is summarized as follows:

- Neglecting tidal velocity leads to underestimation of the computed long-shore current for the case of $f_w = 0.06$, whereas using $f_w = 0.01$ gives a better agreement between the measured and the computed values in some stations. Including tidal velocity gives a better agreement between the computed and the measured long-shore current, especially for the (average profile + σ) in some stations.

Orbital Velocity (Urms): The model always overestimates the orbital velocity.

Prediction of Morphology for the Egmond Site

The prediction of profile after 5 days is carried out for two cases; case i for a time series of wave heights and case ii for a constant wave height. It can be observed that for both cases

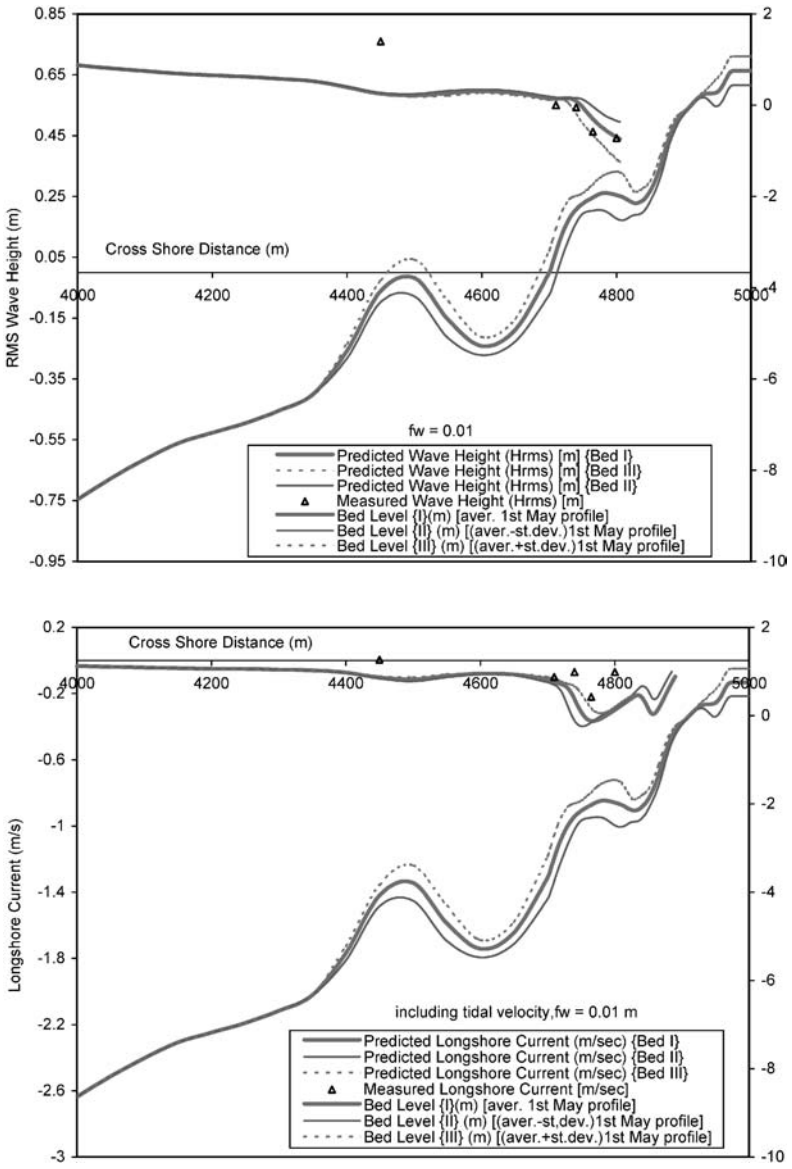

Figure 6. Comparison between measured values and predicted values of wave height and long-shore current using different profiles for Egmond site (case 3, after 78 h).

there was a considerable beach erosion and corresponding sedimentation seaward of the beach and landward migration of the middle bar.

Results of Specific Runs at the Duck Site

Case 1

This case is corresponding to the conditions of high water at 15 October after 19 hours and Hs = 2.5 m. Figure 7 shows the computed and the measured wave height, wave direction, cross-shore current, and long-shore current for the profile of 15 October 1998.

Wave Height: The distribution of wave heights along the profile shows the following:

- The computed values are larger than the measured values about 15% near the most offshore station.
- The computed values are smaller than the measured values about 10% near the beach.
- Most of wave breaking occurs at shallow depth near the beach. The waves approaching the beach have a height of about 1.0 m, resulting in a wave height of about 0.6 m.

Wave Direction: The plot of the predicted values of wave direction and the measured ones shows the following:

- There is a reasonable agreement between the computed values and the measurements near the most offshore location. On the other hand, there is a deviation between the measured values and the predicted values near the beach.
- The deviation between the measurements and the predicted

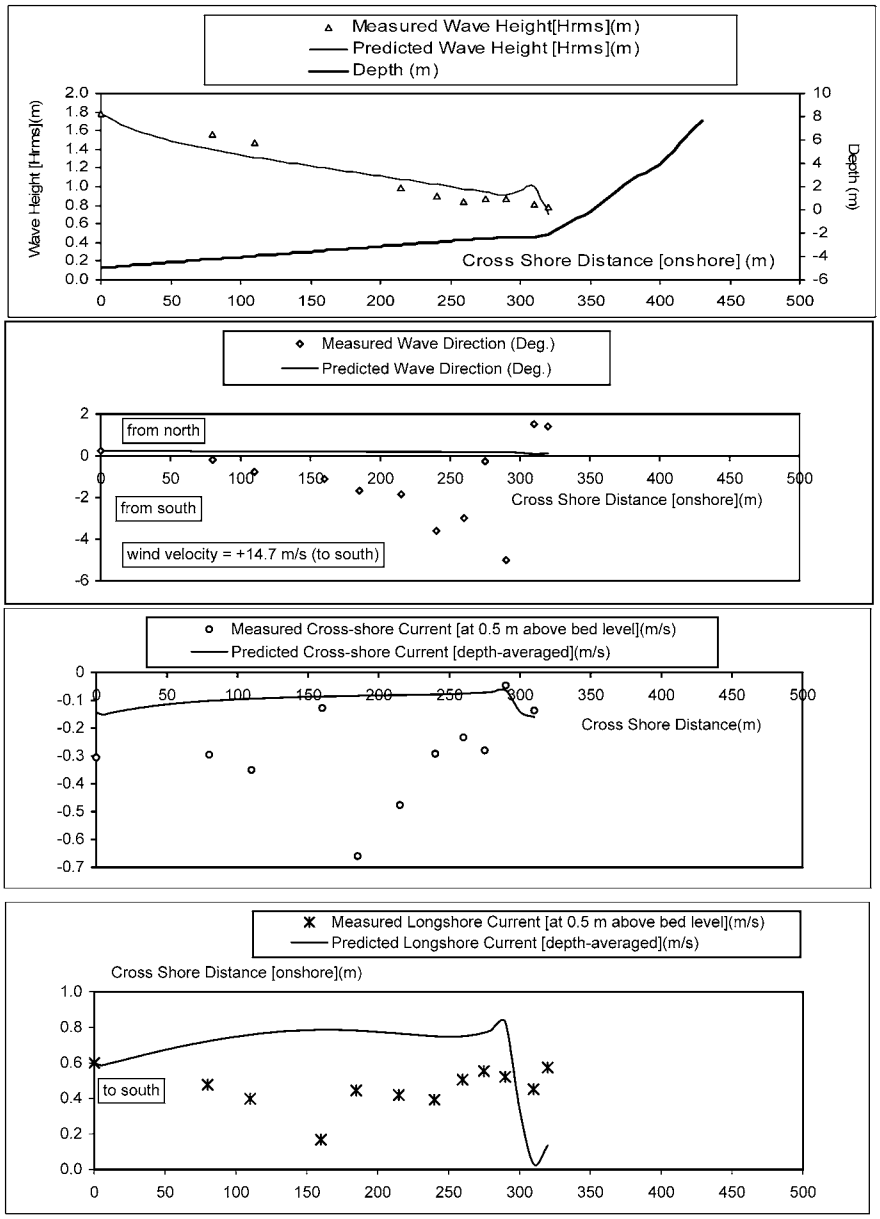

Figure 7. Measured and predicted values of wave height, wave direction, cross-shore current, and long-shore current (Duck site, case 1).

values is partly due to inaccurate measurements, especially in the breaker zone because the turbulence in this active zone of the beach leads to errors in the wave height measurements.

Cross-Shore Current: The distribution of cross-shore current along the profile shows the following:

- There is a deviation between the predicted values by the UNIBEST-TC and the measurements.
- The difference between the measurements and the predicted values could be due to the difference between the measured values, which are at 0.5 m above bed level, and the computed values, which are depth-averaged cross-shore current.

Long-Shore Current: The distribution of long-shore current along the profile shows the following:

- There is a reasonable agreement between the measured values and the predicted values by the model.
- The difference between the measured values and the predicted values is about 30%, and this is partly due to the difference between the measured values, which are at 0.5 m above bed level, and the computed values, which are depth-averaged long-shore current.

Case 2

This case is corresponding to the conditions of low water at 10 October after 1.0 hour and Hs = 0.56 m. Figure 8 gives the computed and the measured wave height, wave direction,

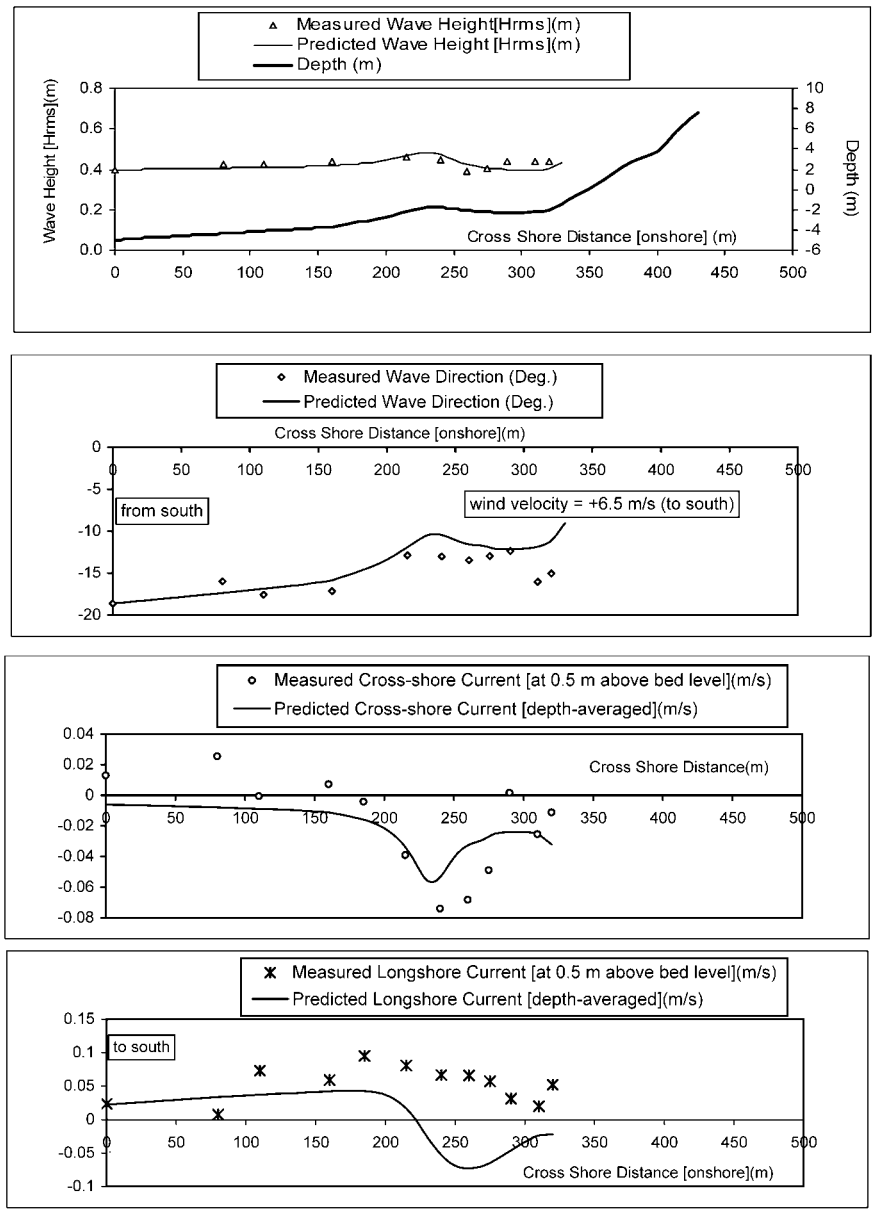

Figure 8. Measured and predicted values of wave height, wave direction, cross-shore current, and long-shore current (Duck site, case 2).

cross-shore current, and long-shore current for the profile of 10 October 1998.

Wave Height: The distribution of wave heights along the profile shows the following:

- There is a good agreement between the measurements and the predicted values by the model at most locations.
- The difference between the computed values and the measured value is within 5%.
- Most of wave breaking occurs at the shallow depth where the depth is about 2.0 m. The waves approaching the beach have a height of about 0.45 m, resulting in a wave height of about 0.35 m.

Wave Direction: The plot of the predicted values of wave direction and the measured ones shows the following:

- There is a good agreement between the computed values and the measurements at most locations.
- The difference between the computed values and the measured values are within 10%.

Cross-Shore Current: The distribution of cross-shore current along the profile shows the following:

- There is a deviation between the predicted values by the model and the measurements.
- The difference between the measurements and the predicted values is within 15%.

Long-Shore Current: The distribution of long-shore current along the profile shows the following:

- There is a deviation between the measured values and the predicted values by the model.
- The difference between the measured values and the predicted values could be partly due to the difference between the measured values, which are at 0.5 m above bed level, and the computed values, which are depth-averaged long-shore current. In addition, the accuracy of the measurements is questionable.

Case 3

This case is corresponding to the conditions of high water at 24 September after 7.0 hours and Hs = 0.75 m. Figure 9 shows the computed and the measured wave height, wave direction, cross-shore current, and long-shore current for the profile of 24 September 1998.

Wave Height: The distribution of wave heights along the profile shows the following:

- There is a good agreement between the computed and the measured values.
- The difference between the computed values and the measured values is within 2%.
- Most of wave breaking occurs above the inner bar. The waves approaching the beach have a height of about 0.58 m, resulting in a wave height of about 0.5 m.

Wave Direction: The plot of the predicted values of wave direction and the measured ones shows the following:

- There is a good agreement between the computed values and the measurements at all locations.
- The difference between the measured values and the predicted values is about 2%.

Cross-Shore Current: The distribution of cross-shore current along the profile shows that there is a deviation between the predicted values by the model and the measurements.

Long-Shore Current: The distribution of long-shore current along the profile shows that there is a deviation between the measured values and the predicted values by the model.

Case 4

This case is corresponding to the conditions of low water at 26 September after 1.0 hour and Hs = 0.67 m. Figure 10 gives the computed and the measured wave height, wave direction, cross-shore current, and long-shore current for the profile of 26 September 1998.

Wave Height: The distribution of wave heights along the profile shows the following:

- There is a good agreement between the measurements and the predicted values by the model at most locations.
- The difference between the computed values and the measured values is within 5%.
- Most of wave breaking occurs above the outer bar where the depth is about 2.0 m. The waves approaching the bar have a height of about 0.5 m, resulting in a wave height of about 0.4 m.

Wave Direction: The plot of the predicted values of wave direction and the measured ones shows the following:

- There is a good agreement between the computed values and the measurements at most locations.
- The difference between the computed values and the measured values is within 5%.

Cross-Shore Current: The distribution of cross-shore current along the profile shows that there is a deviation between the predicted values by the model and the measurements.

Long-Shore Current: The distribution of long-shore current along the profile shows that there is a deviation between the measured values and the predicted values by the model.

Prediction of Morphology for the Duck Site

The plots of the measured profiles and the predicted ones for two periods (21–26 September 1998 and 10–20 October 1998) are given in Figures 11 and 12. In Figure 11, it can be noticed that there is flattening and slight seaward migration of the inner bar, while the measured profile shows landward migration of the bar. Figure 12 shows that the predicted profile by UNIBEST-TC gives considerable beach erosion and corresponding sedimentation seaward of the beach and slight offshore migration of the inner bar, while the measured profile shows a larger offshore migration of the bar.

DISCUSSION

Discussion of the Validation of UNIBEST-TC Wave Model

Wave Height: Using three profiles at the Egmond site shows that there is a good agreement between the computed values and the measured values by considering the (average profile + σ). It can be concluded that the prediction of wave heights is good for both sites (Egmond and Duck). There is a good agreement between the predicted wave heights by the UNIBEST-TC model and the measurements.

Wave Direction: Wave direction predicted by the UNIBEST-TC wave model is in a good agreement with the measurements for both sites (Egmond and Duck). It can be concluded that the prediction of wave directions by the UNIBEST-TC model is satisfactory.

Flow Model

Cross-Shore Current: For the Egmond site, there is a deviation between the measured values and the computed values of cross-shore current by the UNIBEST-TC model for both cases of calculation: (i) including tidal velocity and (ii) excluding tidal velocity. The model prediction for cross-shore current is not accurate enough because the UNIBEST-TC model does not include the 3D effect of rip current at the Egmond site. In addition, there is a deviation between the predicted values by UNIBEST-TC and the measurements for the Duck site. The deviation between the measured values and the predicted ones at the Duck site is partly due to the difference between the measured values, which are at 0.5 m above bed level, and the computed values, which are depth-averaged cross-shore current.

Long-Shore Current: The agreement between computed and measured long-shore current is generally reasonable at

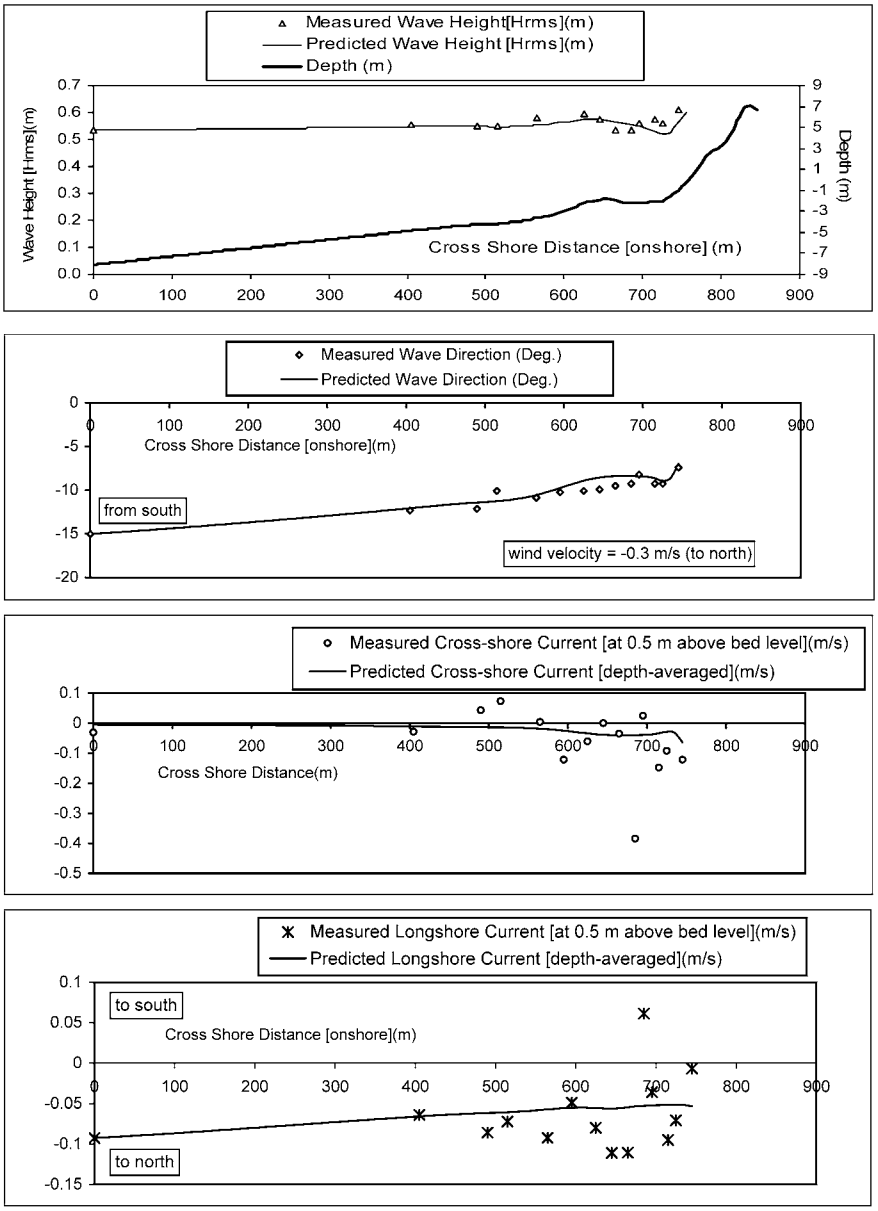

Figure 9. Measured and predicted values of wave height, wave direction, cross-shore current, and long-shore current (Duck site, case 3).

the Egmond site. The difference between the measured and the predicted values is partly due to the difference between the measured long-shore velocity, which was at 0.25 m above bed level, and the predicted long-shore velocity by the model, which is depth-averaged long-shore velocity. Long-shore current predicted by the UNIBEST-TC wave model is not in a good agreement with the measurements for the Duck site. The deviation between the measurements and the predicted values at the Duck site is partly due to inaccurate measurements, especially in the breaker zone because the turbulence in this active zone of the beach leads to errors in the measurements. Also the difference between the measured values, which are at 0.5 m above bed level, and the computed values, which are depth-averaged long-shore current, is another factor.

Orbital Velocity Model

The model always overestimates the orbital velocity for the Egmond site. There is a deviation between the measured values and the computed values because the orbital velocity gives cross-shore activity and improvement of the used theory for calculating the effect of wave asymmetry is needed. Also, it can be concluded that the friction factor *fw* (the friction factor for wave dissipation due to bottom roughness) has an insignificant role in the prediction of Urms (root-mean-square orbital velocity).

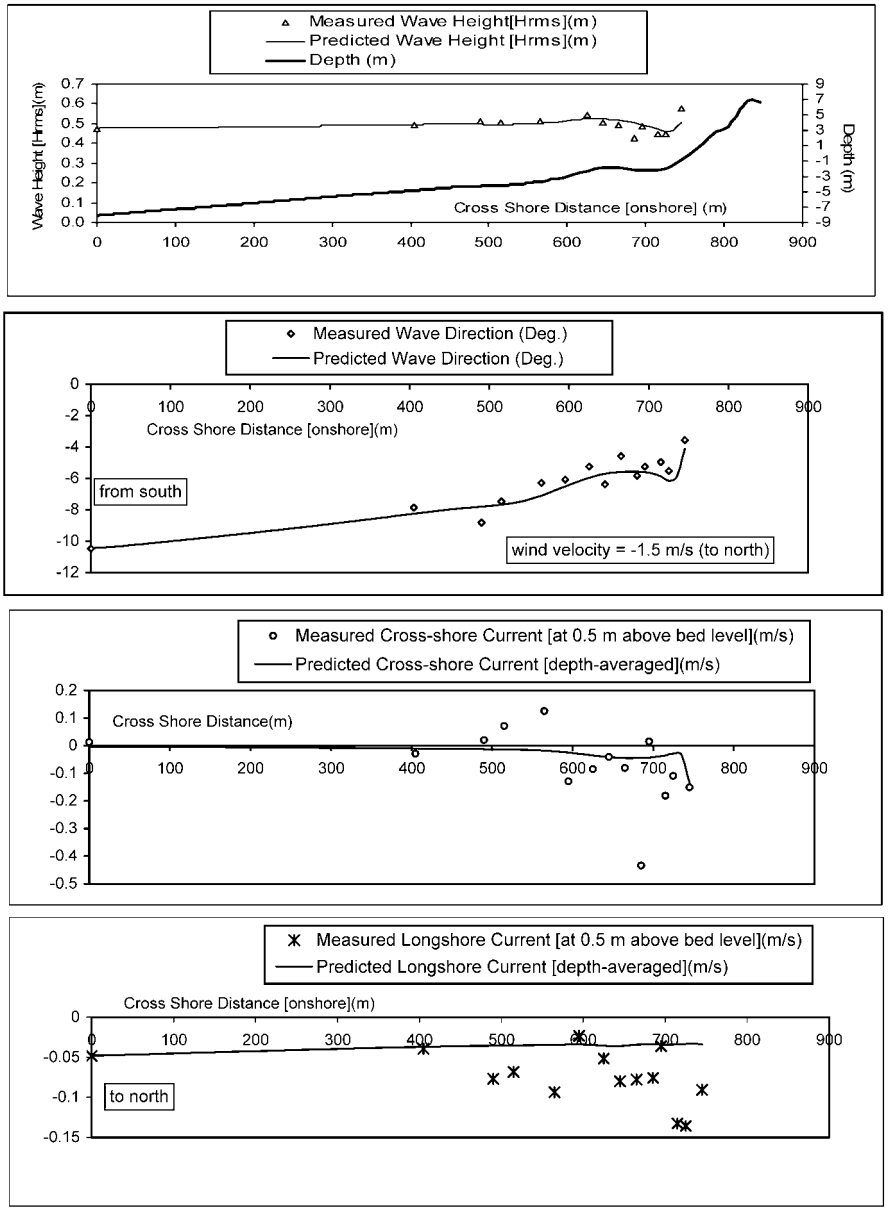

Figure 10. Measured and predicted values of wave height, wave direction, cross-shore current, and long-shore current (Duck site, case 4).

Prediction of Morphology

The prediction of morphology is carried out for the two sites (Egmond site and Duck site). It is observed that, on relatively small scales, opposite morphological behavior is present. Therefore, morphodynamic profile modeling requires a representative characteristic bottom profile.

CONCLUSIONS

The main findings of the present study are summarized in the following conclusions:

- The model is capable of predicting wave height and wave direction for both sites (Egmond site and Duck site).
- The prediction of long-shore current is reasonable for the Egmond site but is unsatisfactory for the Duck site. In addition, there is a deviation between the measured values and the predicted values of the cross-shore current.
- The difference between the measured and the predicted values for the long-shore current and cross-shore current is partly due to the difference between the measured values, which are at a certain depth, and the predicted values, which are depth-averaged velocity. In addition, the turbulence in the breaker zone leads to errors in the measurements, which could be another factor.
- The assumption that the long-shore current can be determined locally does not seem to hold. It is therefore recom-

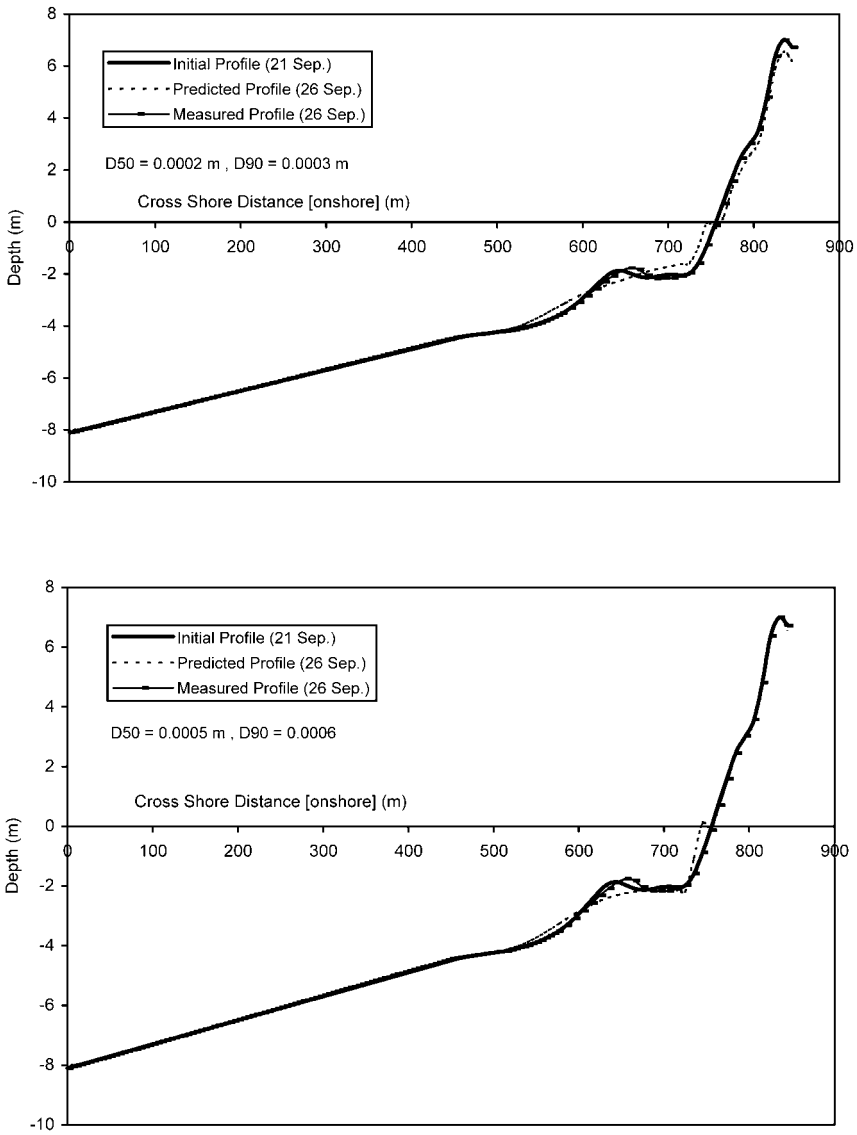

Figure 11. Cross-shore profile evolution at the Duck site during the period 21–26 September.

mended to include the lateral mixing of momentum, which will result in lateral shear stresses and hence reduce the sensitivity of the long-shore current to the forcing due to wave breaking.

- Further investigations should be done in order to improve the model for mass flux due to surface rollers and nonbreaking progressive waves in the surf zone and the model for the return flow due to those mass fluxes.
- Bed forms have a significant effect on sediment transport calculations. Therefore, it is recommended to include this feature in UNIBEST-TC.
- Inclusion of cross-shore variation of sediment properties would improve the transport model.
- The orbital velocity model is always overestimated. Therefore, the relation between wave envelope for short waves and bound long waves needs to be revised.
- Morphodynamic profile modeling requires a representative characteristic bottom profile. It is shown in the present study that, on relatively small scales, opposite morphological behavior is present.
- To achieve a qualitative data for the calibration of the model, it is suggested that field measurements include error ranges. The error ranges should include effects such as the deviations of the applied theories on the processing of the measured signals. Furthermore, the effect of small variations of the water depth on the processing of the signals should also be taken into account.

ACKNOWLEDGMENTS

The author carried out the present study during his MSc work at Delft Hydraulics under the supervision of Prof. Leo

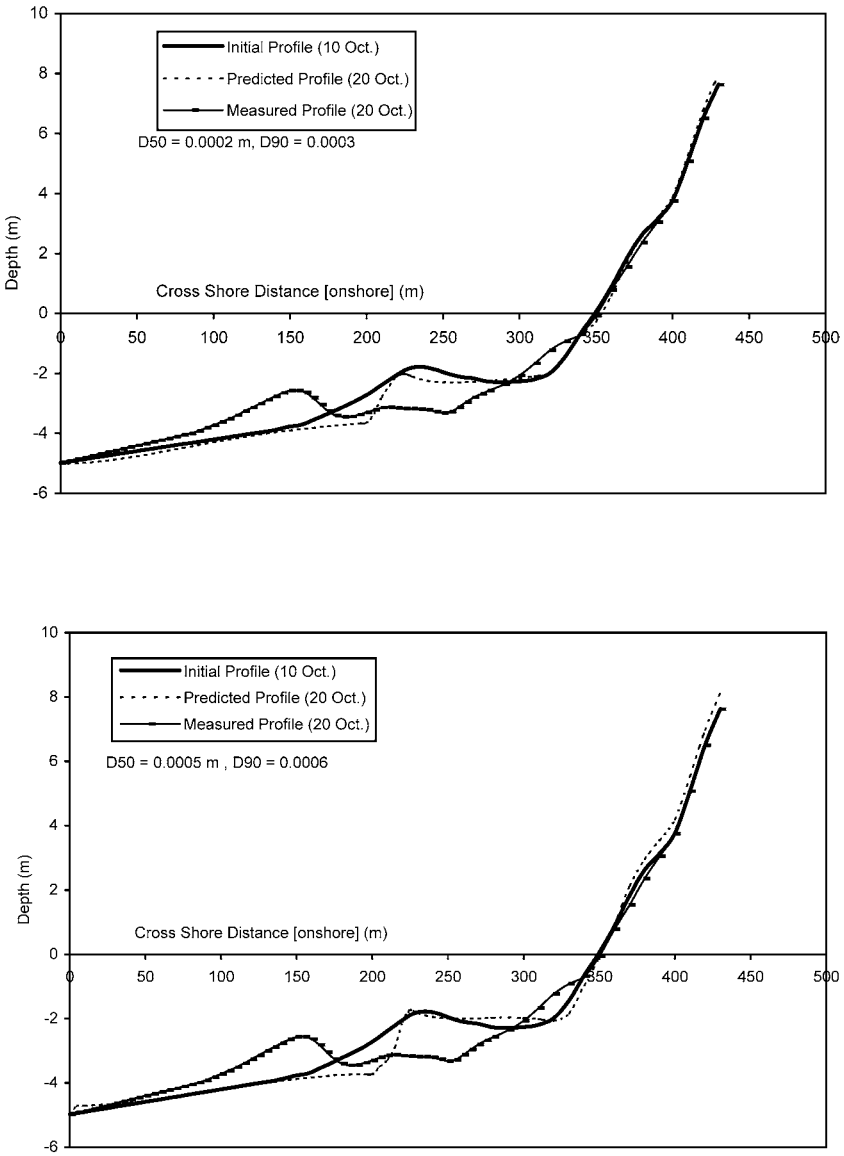

Figure 12. Cross-shore profile evolution at the Duck site during the period 10–20 October.

C. van Rijn and Ir. Walstra. The author would like to express his deep gratitude to Prof. van Rijn and Ir. Walstra for their help and guide during this research. The author would like to thank Prof. Charlie Finkl for his support.

LITERATURE CITED

BAILARD, J.A., 1981. An energetic total load sediment transport model for a plane sloping beaches. *Journal of Geophysical Research,* 86, 10938–10954.

BATTJES, J.A. and JANSSEN, J.P.F.M, 1978. Energy loss and set-up due to breaking in random waves. *In: Proceedings of the 16th International Conference on Coastal Engineering.* New York: ASCE, pp. 569–587.

BIRKEMIER, W.A., 1984. Time scales of near-shore profile changes. *In: 19th International Conference on Coastal Engineering.* Houston: ASCE, pp. 71507–71521.

BOSBOOM, J.; AARINKHOF, S.G.J., RENIERS, A.J.H.M., ROELVINK, J.A., and WALSTRA, D.J.R., 1997. UNIBEST-TC version 2.0: overview of model formulations. Report No. H2305.42, WL/Delft Hydraulics.

DEIGAARD, R. and FREDSOE, J., 1989. Shear stress distribution in dissipative water waves. *Coastal Engineering,* 113, 357–378.

DEIGAARD, R.; FREDSOE, J., and HEDEGAARD, I.B., 1986. Suspended sediment in the surf zone. *Journal of Waterway, Ports, Coastal and Ocean Engineering,* 112(3), 115–128.

DE VRIEND H.J. and STIVE M.J.F., 1987. Quasi-3D modeling of near shore currents. *Coastal Engineering,* 11(5–6), 565–601.

ENGELUND, F. and FREDSOE, J., 1976. A sediment transport model for straight alluvial channels. *Nordic Hydrology,* 7, 293–306.

FORNERIO, S.M.P. and HAMM L., 1992. Numerical modeling of finite amplitude wave shoaling in presence of currents. *In: Hydraulic engineering Software IV, Fluid Flow Modeling Computational Mechanics Publication.* Southhampton, United Kingdom, pp. 587–598.

FREDSOE, J., 1984. Turbulent boundary layer in wave and current motion. *Journal of Hydraulic Engineering,* 110(8), 1103–1120.

HEDEGAARD, I.B.; DEIGAARD, R., and FREDSOE J., 1991. Onshore/offshore sediment transport and morphological modeling of coastal profiles. *In: Proceedings of ASCE, Special Conference on Coastal Sediments.* Seattle: ASCE, pp. 303–309.

ISOBE, M. and HORIKAWA, K., 1982. Study on water particle velocities of shoaling and breaking waves. *Coastal Engineering in Japan,* 25, 1385–1404.

LARSON, M. and KRAUS, N.C., 1992. Analysis of cross-shore movement of natural long-shore bars and material placed to create long-shore bars. Report 32463, US Corps of Engineers, Vicksburg, Mississippi.

LARSON, M. and KRAUS, N.C., 1994. Temporal and spatial scales of beach profile change, Duck, North Carolina, USA. *Marine Geology,* 117, 75–94.

LEPEINTRE, F.; GEST, B., HERVOUET, J.M., and PECHON, P., 1991. MITHRIDATE (former name of TELEMAC-3D): A finite element code to solve 3D surface flow problem. *In: Second International Conference on Computer Modeling in Ocean Engineering.* Barcelona: Taylor and Francis.

LIPPMANN, T.C.; HOLMAN, R.A., and HATHAWAY, K.K., 1993. Episodic, non-stationary behavior of a double bar system at Duck, North Carolina, USA, 1986–1991. *Journal of Coastal Research,* 15, 49–75.

LONGUET-HIGGINS, M., 1953. Mass transport in water waves. *Philosophical Transactions of the Royal Society of London Society,* Series A, 245, 535–581.

MASE, H. and IWAGAKI, Y., 1982. Wave height distribution and wave grouping in surf zone. *In: Proceedings of International Conference in Coastal Engineering.* Houston: ASCE, pp. 58–76.

MIZUGUCHI, M., 1982. Individual wave analysis of irregular wave deformation in the near shore zone. *In: Proceedings of International Conference in Coastal Engineering.* New York: ASCE, pp. 485–504.

ROELVINK, J.A. and BROKER, I., 1993. Cross-shore profile models. *Coastal Engineering,* 21(1–3), 163–191.

SAKAI, S.; HIRYAMA, K., and SAEKI, H., 1988. A new parameter for wave breaking with opposing current on sloping bed. *In: Proceedings of International Conference in Coastal Engineering.* New York: ASCE, pp. 1035–1044.

SOUTHGATE, H.N. and NAIRN, R.B., 1993. Deterministic profile modeling of near shore processes. Part 1: Waves and currents. *In: Proceedings of the 19th International Conference on Coastal Engineering.* New York: ASCE, pp. 27–56.

SVENDSEN, I.A., 1984. Wave heights and set-up in surf zone. *Coastal Engineering,* 8, 303–329.

SWART, D.H., 1978. Vocoidal water wave theory, volume 1: Derivation. CSIR Report 357. Stellenbosch: National Research Institute for Oceanography.

VAN RIJN, L.C.; RENIERS, A.J.HM., ZITMAN, T., and RIBBERINK, J.S., 1995. Yearly average sand transport at the 20 m and 8 m NAP depth contours of the JARKUS-profiles 14,40,76 and 103. WL/Delft Hydraulics Report H1887.

WANTANABE, A.; HARA, T., and HORIKAWA, K., 1984. Study on braking condition for compound wave trains. *Coastal Engineering in Japan,* 17, 71–82.

WANTANABE, A. and DIBANJNIA, M., 1988. A numerical model of wave deformation in surf zone. *In: Proceedings of Coastal Engineering Conference.* New York: ASCE, pp. 578–587.

WEGGEL, J.R., 1972. Maximum breaker height for design. *In: Proceedings of International Conference on Coastal Engineering.* New York: ASCE, pp. 419–432.